J Comput Aided Mol Des (2006) 20:449–461
DOI 10.1007/s10822-006-9064-0

ORIGINAL PAPER

Inactive and active states and supramolecular organization of GPCRs: insights from computational modeling

Francesca Fanelli · Pier G. De Benedetti

Received: 14 June 2006 / Accepted: 4 August 2006 / Published online: 29 September 2006

Abstract Herein we make an overview of the results of our computational experiments aimed at gaining insight into the molecular mechanisms of GPCR functioning either in their normal conditions or when hit by gain-of-function or loss-of-function mutations. Molecular simulations of a number of GPCRs in their wild type and mutated as well as free and ligand-bound forms were instrumental in inferring the structural features, which differentiate the mutation- and ligand-induced active from the inactive states. These features essentially reside in the interaction pattern of the E/DRY arginine and in the degree of solvent exposure of selected cytosolic domains. Indeed, the active states differ from the inactive ones in the weakening of the interactions made by the highly conserved arginine and in the increase in solvent accessibility of the cytosolic interface between helices 3 and 6. Where possible, the structural hallmarks of the active and inactive receptor states are translated into molecular descriptors useful for in silico functional screening of novel receptor mutants or ligands. Computational modeling of the supramolecular organization of GPCRs and their intracellular partners is the current challenge toward a deep understanding of their functioning mechanisms.

F. Fanelli (✉)
Dulbecco Telethon Institute, University of Modena and Reggio Emilia, Via Campi 183, 41100 Modena, Italy
e-mail: fanelli@unimo.it

P. G. De Benedetti · F. Fanelli
Department of Chemistry, University of Modena and Reggio Emilia, Via Campi 183, 41100 Modena, Italy

Keywords GPCRs · G proteins · Constitutively active mutants · Comparative modeling · Molecular dynamics · Protein–protein docking · Molecular recognition

Introduction

GPCRs constitute the largest superfamily of membrane proteins known to date and regulate all aspects of cell activity by transmitting extracellular signals inside the cell (reviewed in refs [1–5]). They have an enormous physiological and biomedical relevance being the primary site of action of many of today's life-saving drugs and the most promising targets for those to be developed in the future (reviewed in refs [1–5]).

The classical idea that GPCRs function as monomeric entities has been unsettled by the emerging evidence that GPCRs exist as homo- and heterodimers/oligomers (reviewed in refs [6–16]) Thus, regulated protein–protein interactions are key features of many aspects of GPCR function and there is now increasing evidence for GPCRs acting as part of multicomponent units comprising a variety of signaling and scaffolding molecules [4, 17].

GPCRs are allosteric proteins, which exist as complex statistical conformation ensembles [18–20]. They hold regions at high stability (i.e., low flexibility) and regions at low stability (i.e., high flexibility) that communicate with each other, even if distal. The functional properties of a GPCR are related to the distribution of states within the native ensemble [19, 20]. Such distribution is differently affected by ligands and/or interacting proteins and/or amino acid mutations [19, 20]. Of course, the different oligomeric states of a GPCR

may contribute to differentiate the distribution of the receptor states.

Difficulties in understanding GPCR functioning mechanisms are also related to the lack of high-resolution information on these proteins. In fact, the unique atomistic models resolved so far, the crystal structures of rhodopsin in the dark state, became available only 6 years ago [21].

Computational modeling of GPCRs has, hence, to face the difficulties due to the lack of high-resolution information even on the ground state and the need to provide a stochastic description of these systems also for rational drug design purposes.

In this article, we make a brief review of the main achievements of our comparative studies based on the integration between computational and in vitro experiments and aimed at gaining insight into different aspects of GPCR function (reviewed also in ref. [22]).

Single molecule computational modeling of GPCRs

Structural features of mutation-induced active and non-active receptor states

Computational modeling of mutation-induced active and non-active states of GPCRs was focused on the α_{1b}-adrenergic receptor (α_{1b}-AR) [23, 24], the luteinizing hormone receptor (LHR) [25–30] and, to a lesser extent, on oxytocin receptor (OTR) [31] (reviewed also in refs. [22, 32]).

The computational approach, developed on previous ab initio receptor models, is aimed at inferring the structural hallmarks of functionally different receptor states through extensive comparative Molecular Dynamics (MD) simulations on the structures of the wild type and of the inactive and constitutively active receptor mutants. The approach consists of generating a large number of average receptor configurations following MD simulations of the wild type and the mutated forms of a common input structure. A comparative analysis of such average arrangements is then carried out focusing on the few but significant structural features, which are shared in common by the majority of the mutant structures with similar functionality and which make the difference between active and non-active forms [33–37]. If possible, the structural hallmarks of the active and non-active states are translated into molecular descriptors useful for in silico functional screening of novel receptor mutants. This strategy is thought to overcome, at least in part, the drawbacks related to the low resolution of the computational models and the approximations and simplifications in the computational setup.

The first target of computational experiments was the α_{1b}-AR [22–24, 34–39]. Computational modeling of all the 19 possible replacements of A293(6.34) (the numbering in parenthesis follows the numbering scheme by Ballesteros and Weinstein [40]) in the α_{1b}-AR, characterized by variable levels of constitutive activity [41], highlighted the role of the E/DRY conserved motif in regulating the agonist-independent transition from the inactive to the active receptor states [37]. In the inactive states, represented by the wild type and the non-active A293(6.34) mutants, R143(3.50), of the conserved E/DRY motif, was found engaged in H-bonding and van der Waals attractive interactions with polar conserved amino acids in H2 and H7 (the letter ''H'' stands for ''helix''). These studies were, therefore, suggestive of an H-bonding network of conserved amino acids as constitutive structural feature of the non-active receptor states, consistent with the results of previous computations on more simplified models of the same receptor [42, 43]. The release of the H-bonding network involving R143(3.50) and the cluster of conserved polar amino acids was found to be a common feature to all the constitutively active mutants (CAMs) at A293(6.34) [37]. Computer simulations suggested also a potential mechanism of regulation of GPCR function via changes in the protonation state of the aspartate of the E/DRY motif, with the protonated form being associated with the active states [37]. This hypothesis was inferred from the observation that reprotonation of D142(3.49) conferred to the α_{1b}-AR the same average structural features shown by the highly active mutants of A293(6.34). The idea that reprotonation of D3.49 was the perturbation, other than mutation, able to trigger agonist-independent active states of the wild-type α_{1b}-AR was also supported by the results of in silico mutagenesis showing that replacements of D142(3.49) with neutral amino acids would give the structural features of the active states to the receptor [36, 37]. Predictions of computational modeling were validated by the experimental findings that the irreversible reprotonation, following mutation, of D142(3.49) led to constitutively active forms of the α_{1b}-AR [36, 37]. In this respect, the D142(3.49)A mutant was the first example in the literature of computational design of a constitutively active GPCR mutant [37]. These inferences are consistent with the knowledge that the homologous glutamate in rhodopsin is involved in proton uptake from the cytosol (reviewed in ref. [44]). In vitro and in silico substitution of D142(3.49) with 19 different amino acids led to the conclusions that the hydrophilic/

hydrophobic character of D142(3.49), which could be regulated by deprotonation/reprotonation of its side chain, is an important modulator of the transition between the inactive and active states of the α_{1b}-AR [36].

Upgrading the α_{1b}-AR model, to incorporate advances in structural determination of rhodopsin, strengthened the hypothesis that the E/DRY motif might play a role in maintaining the inactive state of the receptor, while introducing novel structural hallmarks of the active and non-active states, such as the degree of solvent accessibilities of selected cytosolic domains, including the second and third intracellular loops (I2 and I3, respectively) and the cytosolic extensions of H3 and H6. These domains, in fact, underwent solvent exposure on going from the non-active to the active receptor forms and were, hence, suggested to hold potential recognition points for the G protein [34, 35, 38]. These results found consistency with the results of automatic docking simulations of the wild type α_{1b}-AR and two CAMs (i.e., D142(3.49)A and A293(6.34)E) with different heterotrimeric G proteins [34, 35].

In more recent studies, computational modeling of more than 100 single and double mutants of the α_{1b}-AR by using both the previous ab initio model and the most recent homology model (i.e., based upon the crystal structure of rhodopsin) made it possible the definition of virtual structures representatives of the agonist-independent active and non-active states [22–24]. Furthermore, critical comparisons between the ''ground state'' models achieved by ab initio and comparative modeling provided new insights into the structural features differentiating the inactive from the active receptor forms, including the interaction pattern of the E/DRY arginine. A feature of the inactive state within the homology model, not shared with the previous ab initio model because of slightly different rotation of H6, is the charge reinforced H-bond between the E/DRY arginine and E289(6.30), predicted to be an additional constraint to the R143(3.50) motion and a link between the cytosolic extensions of H3 and H6. Thus, in the novel ground state model, R143(3.50) is involved in charge reinforced H-bonds with both D142(3.49) and E289(6.30). These interactions are released in the structures of the highly active α_{1b}-AR mutants, suggesting that both the two anionic amino acids stabilize the inactive state of the receptor. The role of the charge-reinforced H-bond between R3.50 and E6.30 in maintaining the inactive states of GPCRs has been overemphasized by a number of computational and in vitro experiments [23, 24, 28–30, 45–49]. However, the significantly lower conservation of the glutamate/aspartate at position 6.30 (i.e., 32%) compared to the glutamate/aspartate at 3.49 (i.e., 86%) [50] makes its potential role valid only for a very limited number of GPCRs. Computations on the μ opioid receptor [51], on the melanine-concentrating hormone receptors (MCHRs) [52], and on OTR [31] suggested that, in the absence of a conserved glutamate/aspartate at position 6.30, other amino acids in the cytosolic extension of H6 may contribute to create H-bonding interactions with the E/DRY arginine. These amino acids include T6.34, for the μ opioid receptor [51], T6.30, for MCHR1 [52], and T6.33, for OTR [31].

In vitro and in silico mutagenesis of the amino acids lying at the H3–H6 interface also suggested that the role of the amino acids at the cytosolic half of H6 in the α_{1b}-AR activation is strongly correlated with the extent of their structural/dynamic connection with H3 and the arginine of the E/DRY sequence [23].

Critical comparisons of the interpretative and predictive abilities of the previous ab initio and the novel homology models of the α_{1b}-AR as well as of LHR and OTR suggest that the homology models can be considered advancements over the previous ab initio models, which, however, have been extremely useful for developing the computational approach.

As for the LHR, MD simulations on a novel rhodopsin-based receptor model of almost all the spontaneous pathogenic activating and inactivating mutations discovered so far strengthened the role of the cytosolic extensions of H3 and H6 as the targets of the structural modifications induced by the activating mutations. In fact, consistent with previous computational results on the ab initio LHR model, a common and peculiar feature to all the CAMs and not to the inactive forms is the opening of a cytosolic crevice between I2 and I3 and between H3 and H6 [25–30]. This structural effect was properly accounted for by the solvent accessible surface area (SAS) computed over selected amino acids including the E/DRY arginine [i.e., R464(3.50), T467(3.53), I468(3.54), and K563(6.29)]. The composite SAS index, indeed, proved to be an effective hallmark of the functional receptor state, being lower than 50 $Å^2$ in the inactive forms and higher than 50 $Å^2$ in the active ones [27–29] (Fig. 1). It was, therefore, successfully probed in its ability to predict the functional behavior (i.e., active and non-active) of artificial mutants of the LHR, proving an improved predictive ability compared to the SAS index defined on the previous ab initio model [28–30].

Another feature of the most active LHR mutants, as inferred from the latest computational analysis, is the weakening of either one or both the charge-reinforced H-bonding interactions found in the wild type between R464(3.50), of the E/DRY motif, and both E463(3.49)

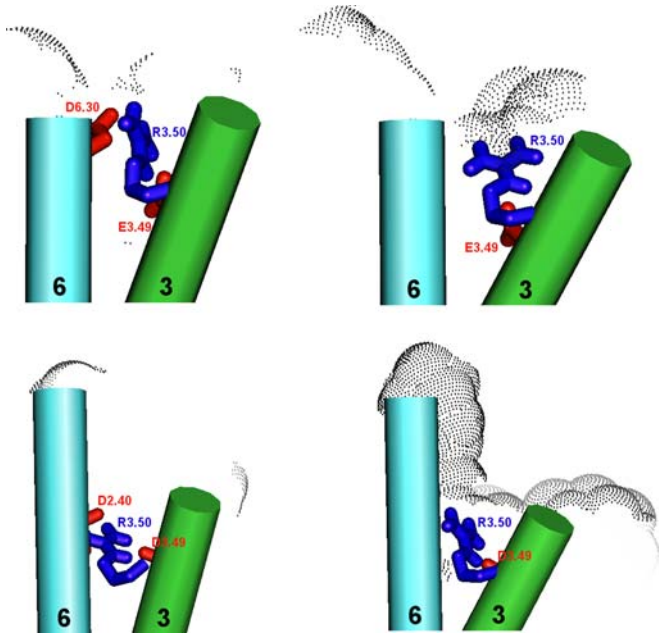

Fig. 1 Top. Cytosolic ends of H3 and H6 extracted from the average minimized structures of the wild type (*left*) and D564G CAM (*right*) forms of LHR. The interaction pattern of R3.50 is shown. *Dots* indicate the SAS computed over R464(3.50), T467(3.53), I468(3.54), and K563(6.29). SAS is 28 $Å^2$, for the wild type, and 120 $Å^2$, for D564G. Bottom. Cytosolic ends of H3 and H6 extracted from the structures averaged over the last 100 ps of 1 ns trajectories of the wild-type MCHR1 in its empty (left) and MCH-bound (right) forms. The interaction pattern of R3.50 is shown. Dots indicate the SAS computed over N76(2.37), R141(3.50), K153 (in I2), I247(6.26), and T251(6.30). SAS is 23 $Å^2$, for the empty wild type, and 254 $Å^2$, for the MCH-MCHR1 complex

and D564(6.30) (Fig. 1). These results strengthen the hypothesis that both the coulombic interactions involving the E/DRY arginine, inherited from rhodopsin structure, contribute to maintain the inactive state of the LHR.

The extensive in vitro and in silico mutagnesis experiments, characterized by the generation of a number of single and multiple mutants of selected activating mutation sites, allowed us to infer the structural triggers of the constitutive activation by mutations of M398(2.43), L457(3.43), and D578(6.44). The trigger of the activation by M398(2.43) mutations was suggested to be size reduction of the replacing side chain [29]. This effect is associated with reduction in the strength of the interaction between the replacing amino acid and the highly conserved tyrosine of the NPxxY motif in H7. Differently from M2.43, only cationic amino acid substitutions for L457(3.43) are able to trigger constitutive activity [25, 30]. Computational modeling suggested that, in this case, the activation trigger is a salt bridge between positions 3.43 and 6.44. In the L457(3.43)R mutant, the formation of such an inter-helical salt bridge is allowed by the presence of D578(6.44) in the proximity to the mutated position. The L457(3.43)D and D578(6.44)R single mutants, which cannot allow for the interhelical salt bridge, hold a SAS index below the threshold and, consistently, are non-constitutively active. In contrast, the combination of the two non-active mutants in the L457(3.43)D/D578(6.44)R mutant, which reintroduces two opposite charges at positions 3.43 and 6.44, restores the interhelical salt bridge, increases the SAS index above the threshold and, consistently, results in constitutive activation. Intriguingly, the formation of such an ionic lock between the transmembrane (TM) portions of H3 and H6 favors hormone-independent LHR activation but impairs hormone-induced activation. As for D578(6.44), spontaneous and artificial mutations of this aspartate are suggested to perturb the inter-helical H-bond found in the wild type between the mutation site and N615(7.45) [28].

In summary, computational modeling of a number of spontaneously occurring single and multiple LHR mutants suggests that the ultimate effects of activating mutations is the weakening of either one or both the salt bridges involving the E/DRY arginine and the increase in solvent accessibility of selected amino acids at the cytosolic interface between H3 and H6, including the conserved R3.50. Intriguingly, three of four residues employed for monitoring the increase in solvent accessibility are among the few amino acids essential for Gs coupling, based upon the results of in

vitro alanine scanning mutagenesis of the cytosolic extensions of H3 and H6 and of the whole I2 and I3 (K. Angelova et al., manuscript in preparation). The structural information transfer from the mutation site to the cytosolic interface between H3 and H6 appears to be mediated by the highly conserved polar amino acids in the TM domains, i.e., D2.50, N7.45, N7.49, and Y7.53. This hypothesis was inferred from the observation that the integrity of these amino acids is required for full mutation-induced activation and, consistently, for the structural communication between the mutation site and the environment of the E/DRY motif. This hypothesis is also consistent with the fact that, in the LHR model, the activating mutation sites are, indeed, close to these highly conserved polar amino acids.

In line with computational results on α_{1b}-AR and LHR, molecular simulations of the D136(3.49)N CAM of OTR suggested that the receptor portions close to the E/DRY and NPxxY motifs are particularly susceptible to structural modification in response to activating mutations [31]. Furthermore, simulations suggested that the OT-bound form of wild-type OTR is able to explore more states than the OT-bound form of the D136(3.49)N CAM. This may be due, at least in part, to the possibility that the aspartate at position 3.49 can exist both in the non-protonated (anionic) and protonated (neutral) forms, whereas the asparagine can exist only in the neutral state. All together these features correlate with the higher G-protein coupling promiscuity of the OT-bound form of wild-type OTR as compared to the OT-bound form of the active mutant [31].

Structural features of ligand-induced active and non-active states

Over the last 10 years, we have done extensive studies aimed at investigating the propagation of the structural modifications from the ligand binding site to distal receptor domains, following the docking of selected agonists and antagonists into their cognate receptors [31, 35, 42, 43, 48, 52, 53]. Targets of our study have been different members of family A, including α_{1b}-AR, m3-muscarinic receptor, OTR, 5-HT_{1A} serotonin receptor, MCHR1, and MCHR2 [31, 35, 42, 43, 48, 52, 53].

The employment of different receptors allowed us to infer mechanistic commonalties and differences among significantly different members of the rhodopsin family.

The computational approach was essentially the same as that employed to infer the structural differences between mutation-induced active and non-active receptor states, the only difference being the perturbation introduced in the initial model, i.e., ligand docking in one case and point mutation in the other.

An intriguing inference from the latest docking simulations between agonists/antagonists and different GPCRs was that the same ligand, depending on its interaction modes, can generate different average configurations of the same receptor. These configurations differ from those of the empty receptor forms. On the other hand, comparing a large number of average configurations obtained for the different agonist- and antagonist-receptor complexes following different computational protocols, it was possible to infer similarities in the interaction modes of the different agonists at their cognate receptors [31, 48, 52]. The receptor sites, in which most of such similarities occur, essentially concern selected positions in the extracellular halves of H3, H5, and H6. Computational modeling of the agonist-bound forms of the 5-HT_{1A}, MCH, and OT receptors suggests that these receptor portions hold the key contact points for the ligand moieties responsible for the efficacy [31, 48, 52]. According to extensive computational analyses, hallmarks of the ligand-induced active and non-active forms of the receptors were found to involve R3.50, the arginine of the E/DRY motif, and the cytosolic extensions of H3 and H6. In fact, for the agonist-bound (i.e., active) and the antagonist-bound (i.e., non-active) forms, the establishment of crucial intermolecular interactions (as suggested by experimental evidences) was found, respectively, concurrent with destabilization and reinforcement of the intramolecular interactions that involve the E/DRY arginine in the empty receptor forms [31, 48, 52]. For the MCHRs, other structural changes in the cytosolic domains peculiar to the hormone-bound forms include the opening of a solvent accessible crevice involving I2 and the cytosolic extensions of H3 and H6 [52]. This structural change is properly described by the SAS computed over selected amino acids, including the arginine of the E/DRY motif. The SAS index, which is significantly lower than 100 $Å^2$ in the empty and antagonist-bound receptor forms and significantly higher than 100 $Å^2$ in the agonist-bound forms, proved suitability for in silico functional screening of modified forms of MCH (Fig. 1) [52]. The predictive ability of the SAS index was, in fact, put to the test on mutant forms of the hormone obtained by in silico alanine-scanning mutagenesis of all the 19 amino acids, except for the two cysteines involved in a disulphide bridge [52]. A truncated form of the hormone, lacking the first five amino acids, was considered as well. Each modified form of the hormone was

docked in both the MCHR1 and MCHR2 exactly in the same orientation and conformation selected as input for the wild-type MCH. Docking was followed by MD simulations, according to the same computational protocol employed for the wild-type MCH and for the antagonist, ending up in the calculation of the SAS index on the average minimized ligand-receptor complexes. Consistency between in silico-predicted and in vitro-determined functionalities was obtained, as the SAS indices went below 100 $Å^2$ only for the few MCH mutants with impaired functionality [52]. Interestingly, for both the MCHR subtypes, the SAS indices correctly predicted that deleting the first five amino acids of the hormone does not cause any impairment in functionality [52]. The validity of the approach in functional screening of MCH variants suggests also that two of 19 amino acids, which constitute the hormone, are essential for the structural information transfer from the hormone binding site to the cytosolic domains. In this respect, the role of the remaining amino acids, especially those in the cyclic part, is to provide the crucial amino acids with the essential stereochemistry for productive interaction with the receptor.

An interesting inference from comparative MD simulations of GPCRs differing both in amino acid composition and in the natural agonist (i.e., a small biogenic amine, for the 5-HT_{1A}, and a huge cyclic peptide, for OTR and MCHR) is that a few and overlapping critical interactions are needed for the agonist to trigger the structural information transfer from the extracellular to the intracellular domains of its target receptor. For both the 5-HT_{1A} receptor and two MCHR subtypes, these interactions include an intermolecular salt bridge that allows the crucial aromatic moiety of the agonist to establish the proper interaction with one member of the aromatic cluster in H6 (Fig. 2) [31, 48, 52]. In line with these observations, also for the OT–OTR complexes, the few critical intermolecular interactions essential for the structural information transfer include that between Tyr2 of the agonist and F291(6.51) of the aromatic cluster in H6 [31].

Collectively the results of comparative MD simulations on the three different GPCRs suggest that the agonist-induced chemical information transfer from the extracellular to the cytosolic domains (i.e., vertical information transfer) is mediated by a cluster of aromatic amino acids in H6, i.e., formed by F6.44, W6.48, and F6.51, following ligand interaction with selected amino acids in the extracellular half of the receptor [31, 48, 52]. In detail, the interaction between the aromatic ring of the agonist and F6.51 induces a conformational

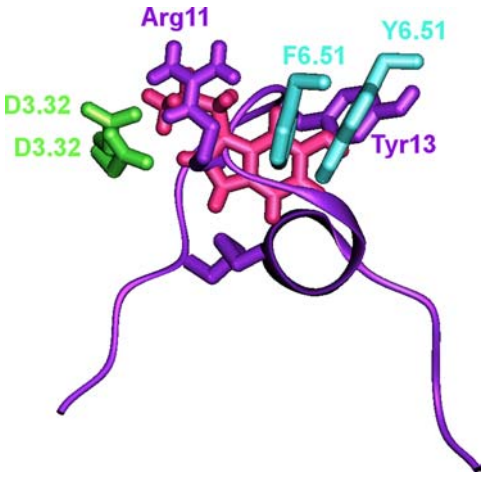

Fig. 2 Superimposition between the average minimized 5-HT-5-HT_{1A} and MCH-MCHR1 complexes. 5-HT is colored in *purple*, whereas MCH is colored in violet. For MCH, the C_a-atoms of the entire peptide and the side-chains of the functionally important Arg11 and Tyr13 are shown. Arg11, like the protonated amino group of 5-HT, makes a charge-reinforced H-bond with D3.32 of the receptor. On the other hand, Tyr13, like the indole moiety of 5-HT, interacts with a member of the aromatic cluster in H6, i.e., Y/F6.51. The side chains of the amino acids at positions 3.32 and 6.51 from both receptors are, therefore, shown, colored according to their location. In this respect, the green color indicates H3, whereas the cyan color indicates H6

change of W6.48, which looses its original interaction with N7.45 and moves from H7 toward H5, consistent with the results of UV determination on rhodopsin [54]. These changes are concurrent with a significant reduction in the bend at the highly conserved P6.50, as compared to the empty and the antagonist-bound receptor forms, consistent with the results of conformational sampling on the isolated H6 of the α_2–AR and the CB1 receptor and restrained MD simulations on an almost complete model of the α_2-AR [55–57]. These results also agree with the computer simulation- and experiment-based hypothesis that GPCR activation would significantly diminish the kink at P6.50 [58]. The straightening of H6 is one of the features of the agonist-bound forms correlated with weakening of the interactions made by R3.50, of the E/DRY motif. Another common feature to the agonist-bound forms of the simulated receptors is the release of the interaction found in the inactive forms between Y7.53, of the NPxxY motif, and a conserved phenylalanine in H8. This is particularly true for the computational models of the two MCHR subtypes, whose agonist-bound forms are characterized by the approaching of H8 to the cytosolic extension of H3 [52]. Thus, the results of our computational experiments highlight a structural connection between the E/DRY and the NPxxY motifs, consistent with in vitro evidence that

the NPxxY(x)$_{5,6}$F and E/DRY motifs provide, in concert, a dual control of the activating structural changes in the photoreceptor [59].

Agonist binding, especially in the cases of peptide receptors like OTR and MCHR, induces significant changes in the arrangements of the extracellular ends of the helix-bundle and in the conformation/orientation of the N-terminus and the second extracellular loop (E2). The latter is strongly involved in interaction with the peptide agonists OT and MCH [31, 52]. The high extent of the structural differences in the putative agonist binding site between free and agonist-bound receptor forms suggests that the role of agonists cannot be limited to a conformation selection but it should also include the triggering of relevant structural changes, unlikely to occur spontaneously in the empty receptor form. These inferences, which should be taken with caution given the indeterminations in the receptor models, are consistent with recent advances in the thermodynamics models of GPCR function [19, 20, 60].

Prediction of the supramolecular architecture of GPCRs and their intracellular partners

A significant part of our research over the last 2 years has been concerned with the development of effective computational approaches for predicting the quaternary structure of membrane proteins as well as the receptor-G protein interface [61–63]. Computational experiments also included an extensive probing of the potentialities and limitations of the rigid-body docking algorithm, including its tolerance to changes in the backbone and/or side chain conformations [64–66]. The ultimate goal is to gain insight, at the molecular level, into the architecture of GPCR multi-component functional units made of oligomeric receptors and intracellular proteins.

Computational modeling of receptor–receptor interaction

So far, predictions of the likely interfaces in GPCR dimers have essentially relied on sequence-based methods [67–72]. We have developed a computational protocol for effective predictions of the supramolecular organization of integral TM proteins, starting from the monomer [62]. The approach, which is independent of the size of the system, symmetry information, extension of the water-soluble domains and resolution of the monomer structure, consists of a number of dense docking samplings (by the ZDOCK program [73]), starting from the docking of two identical copies of a given monomer. Each docking run is followed by membrane topology filtering and cluster analysis. Thus, prediction of the native oligomer is accomplished by a number of progressive growing steps, each made of one docking run, filtering, and cluster analysis. In more detail, in each step, the best solutions selected by the docking program as the best in terms of shape complementarity are then subjected to a filter developed ''in-house'', i.e., the membrane topology filter, which discards all the solutions that violate the membrane topology requirements, i.e., all the solutions characterized by a deviation angle from the original z-axis, i.e., tilt angle, and a displacement of the geometrical center along the z-axis, i.e., z-offset, above defined threshold values. For the tilt angle and the z-offset, thresholds of 0.4 rad and 6.0 Å were employed, respectively. This filter generally discards more than 94% of the total solutions provided by each docking run (i.e., 4,000 solutions), thus allowing for an easy individuation of the clusters holding the native-like solutions. These clusters are, in fact, the one or two most populated, and hold also a significantly good membrane topology. The latter is evaluated by means of the MemTop index defined by the following formula $\mathrm{MemTop} = \sqrt{\langle \mathrm{tilt_{nor}} \rangle^2 + \langle Z_{offnor} \rangle^2}$, were $\langle \mathrm{tiltnor} \rangle$ and $\langle Z_{\mathrm{offnor}} \rangle$ are, respectively, the normalized tilt angle and z-offset averaged over all the members of a given cluster. Tilt angle and z-offset normalization was carried out by dividing each value for the respective cut-off, i.e., 0.4 rad, for the tilt angle, and 6.0 Å, for the z-offset. The optimal value for the MemTop index is zero.

The best scored solution(s) from the most populated clusters, characterized also by the best MemTop index, are selected for growing the oligomer. In all the growing steps that succeed the first one, the original monomer behaves as a probe whereas the intermediate oligomer behaves as a target. For cyclic oligomers, ring closure dictates the end of the growth [62].

Benchmarks of the approach were carried out on ten selected oligomeric functional units. In all the test cases, native-like quaternary structures were achieved, i.e., with Root Mean Square Deviations of the C$_\alpha$-atoms (Cα-RMSDs) lower than 2.5 Å from the native oligomer [62].

The effectiveness of the prediction protocol makes it suitable for quaternary structure predictions of other integral membrane proteins, including GPCRs. An attempt in this respect has been already reported, though based on an early and different version of the computational protocol [61]. In detail, integrating the rigid-body docking approach with the results of protein

engineering and FRET and BRET experiments provided insights into the putative interaction interface of D_2R-$A_{2A}R$ heterodimers [61]. The initial models of the two receptors were achieved by comparative modeling, using modified rhodopsin structures as templates. The whole sequences of both receptors were modeled, since dimerization and/or oligomerization might involve also the cytosolic and/or the extracellular domains, as recently suggested for rhodopsin [74]. Nine different average minimized structures of the $A_{2A}R$ were docked with the selected average minimized structure of D_2R. The different $A_{2A}R$ structures share preferential docking modes at the D_2R, which were broadly grouped into two clusters, CLUSTERs 1 and 2. In particular, in the most populated cluster, CLUSTER 1, H5 and/or H6 and the N-terminal portion of I3, from D_2R, respectively, approach H4 and the C-terminal portion of the C-tail, from the $A_{2A}R$. H7 from D_2R may also participate, together with H6, in the contacts with H4 from $A_{2A}R$. A very short but significant portion of the huge I3 from D_2R, i.e., the N-terminal 217–220 amino acid stretch that contains four consecutive arginines (^{217}RRRR^{220}), is frequently involved in the heterodimer interface (Fig. 3) [61]. Some of the four

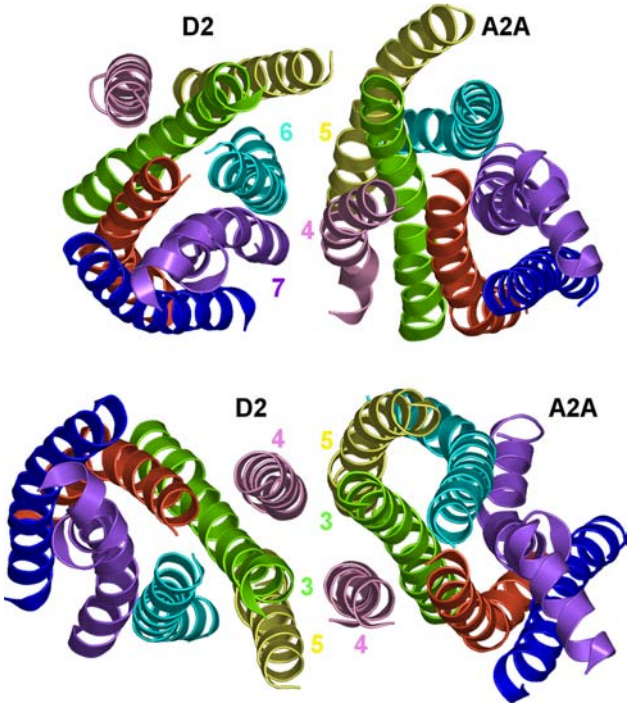

Fig. 3 Examples of the D_2R-$A_{2A}R$ heterodimers belonging to CLUSTER 1 (top) and to CLUSTER 2 (bottom). Only the TM helices are shown seen from the intracellular side in a direction almost perpendicular to the membrane surface. H1–H7 are, respectively, colored in blue, orange, green, pink, yellow, cyan, and violet. H8 is colored in violet as well. Drawings were done by means of the software PYMOL 0.97 (http://pymol.sourceforge.net/)

cationic amino acids in such D_2R stretch are frequently found interacting with D401 and/or D402 from the C-terminal portion of the $A_{2A}R$ C-tail. A few more amino acids from the $A_{2A}R$ C-tail are suggested to participate in the heterodimer interface. Thus, very limited and almost invariant portions of the D_2R I3 and of the $A_{2A}R$ C-tail are likely to mediate D_2R-$A_{2A}R$ contacts. The heterodimer architecture shared by the members of CLUSTER 1 found consistency with the results of BRET experiments using a D_2R/D_1R chimera, which implicated the H5-I3-H6 portion of D_2R in the interaction with $A_{2A}R$ [61]. The predicted interface according to the members of CLUSTER 1 was also consistent with the results of pull-down and mass spectrometry experiments, which suggested that $A_{2A}R$-D_2R heteromerization depends on an electrostatic interaction between an arginine-rich epitope from the I3 of the D_2R (^{217}RRRRKR^{222}) and two adjacent aspartates (D401-402) or a phosphorylated Ser (S374) residue from the C-tail of the $A_{2A}R$ [75].

The second cluster of docking solutions, CLUSTER 2, which is less populated than CLUSTER 1, but characterized by high-docking scores, resembled the intradimer contact model proposed for rhodopsin (Fig. 3) [74]. In this cluster, the heterodimer interface is mainly formed by I2, H4, H3, and H5, from D_2R, and I2, H5, H3, and H4, from $A_{2A}R$. In these dimers, the extracellular end of the interface is made of contacts between aromatic amino acids from E2 and H5. These features could have functional implications, as the extracellular end of H5 is involved in agonist binding. The role of agonist-induced activation on the homo- and heterodimerization of these receptors is still obscure. Recent experimental evidence suggests that it may play a role in the formation of higher-order oligomers, rather than in the formation of dimers, which should be constitutive features of the receptors [61, 76].

Collectively, the results of the simulation of D_2R-$A_{2A}R$ homodimerization suggest that the intermonomer interfaces are made of contacts between the TM helices, whereas the intracellular and extracellular domains contribute to a limited extent.

We are extensively testing the computational approach in quaternary structure predictions of a number of GPCRs, including members of the Amine, Peptide, and Hormone sub-families. Preliminary results on the LHR dimerization, probing different computational models of the wild type receptor, predicted H4–H4, H4–H6, or H5–H6 contact dimers as the most reliable ones. As for the H4–H4 dimer, also H1 and H3, from one monomer, make contacts with H4 from the other monomer [63]. This dimer is characterized by the approaching of the highly conserved W491(4.50) from

both monomers, providing a possible explanation for the fact that W491(4.50), despite its very high conservation, is almost exposed to the lipids in the inactive receptor forms. Interestingly, previous computations highlighted the conserved tryptophan as a marker of the orientation changes of H4 associated with mutation-induced activation of the receptor [29]. In fact, in the structure representative of the ground state, the tryptophan is involved in H-bonding interaction with N400(2.45) (in H2), whereas in the structures of the CAMs it becomes more exposed to the lipids loosing its interaction with N400(2.45) [29]. Collectively, MD simulations on the isolated receptor and computational modeling of LHR homodimerization suggest that mutation-induced LHR activation favors H4–H4 contacts involving the highly conserved tryptophan from both the receptors monomers. These inferences agree with in vitro cysteine cross-linking experiments on the D_2 dopamine receptor, indicating a dynamic involvement of H4 in forming a symmetrical dimer interface [77]. As for the H4–H6 dimer, also H5, from one monomer, participates in the interaction with H4, from the other monomer. Finally, for the H5–H6 dimer, also H7, from one monomer, participates in the interaction with H5, from the other monomer.

In summary, the preliminary results of simulation of GPCR homo- and heterodimerization done so far, emphasize the role of H4–H6, with prominence to H4, in mediating intermonomer interactions, and predict a very limited involvement of the intracellular and extracellular domains.

Computational modeling of the receptor-G protein interface

Very recently, we have also developed a computational protocol for predicting likely receptor-G protein interface. The approach has first been probed on the rhodopsin-transducin (Gt) system and is being now extended to homologous GPCRs and their cognate G proteins [65].

Despite the commonly accepted knowledge that recruitment of Gt would follow rhodopsin activation, experimental evidence that dark rhodopsin and heterotrimeric Gt may exist as a preformed complex have appeared early in the literature, and is ever increasingly emerging [78–82].

We have tested the hypothesis that dark rhodopsin has the potential to recognize Gt [65]. The analysis of the structural complementarity between the cytosolic domains of dark rhodopsin and heterotrimeric Gt was carried out by exhaustively sampling the roto-translational space of one protein with respect to the other. Dark rhodopsin structure (PDB code: 1U19 [83]) was used as the fixed protein (i.e., target), whereas heterotrimeric Gt was allowed to explore all the possible orientations around the cytosolic domains of the target (i.e., probe). The rigid-body docking algorithm ZDOCK was employed, which has already proven effective in structure predictions of protein–protein complexes [84]. While neglecting the conformational changes that may accompany protein–protein interaction is a drawback in some cases, in our study, the rigid-body approximation was rather a requirement as we wanted to investigate whether any reliable complementarity exists between the crystal structure of dark rhodopsin and Gt, independent of possible conformational re-arrangements. However, introduction of differences in the side-chain and/or backbone conformation and/or in the amino acid length of the N- and C-termini of the different G protein subunits was probed as well to infer the degree of tolerance of the rigid-body docking algorithm to such structural changes.

Distance-based filters were employed on the 4,000 best scored solutions provided by each run, in order to minimize false positives. The filtered solutions, which constitute less than 10% of the solutions selected by the docking program, were subjected to cluster analysis and visual inspection of the cluster centers (i.e., the most representative solution in each cluster). The latter analysis, which allowed for a further minimization of false positives, was instrumental in discarding all the solutions that violated the putative membrane topology of the G protein. Acceptable membrane topologies were those, in which the main axis of the N-terminal α-helix of Gt_α (i.e., αN) was almost parallel and close enough to the membrane surface to allow the hydrophobic *N*-acyl and farnesyl modifications of the α- and γ-subunits, respectively, to insert into the membrane. It should be stressed that the complexes from each docking run, which fulfilled at best experimentally based distance constraints and membrane topology requirements, fell amongst the top 23 of the best 4000 solutions. Despite the structural differences in the heterotrimers used as probes in the different docking simulations, the C_α-RMSD of the best scored realistic solutions from each run was close to zero [65]. This proves some tolerance of the ZDOCK algorithm to changes in side chain and/or backbone conformation of the different G protein subunits, providing more strength to the predictions.

In the predicted complex, the C-terminus of Gt_α makes contacts with I2, the cytosolic extensions of H3 and H6, as well as with H8 and the C-terminus of rhodopsin. Furthermore, (a) the $\alpha 3/\beta 5$ loop of Gt_α

interacts with the C-terminus of rhodopsin; (b) the $\alpha 4/\beta 6$ loop of Gt_α makes contacts with both I3 and the C-terminus of rhodopsin; and (c) the C-terminus of rhodopsin is also involved in contacts with the N-terminus of Gt_α and with limited portions of Gt_β (Fig. 4). The functionally important R135(3.50) of the E/DRY motif is almost accessible to the C-terminus of Gt_α already in the dark state. In fact, the C_α–C_α distance between the E/DRY arginine and F350, the last amino acid of Gt_α is 7.9 Å. Therefore, a limited energy minimization of the rhodopsin-Gt complex reveals the possibility for R135 to switch from the intramolecular salt bridge with E247(6.30) to an intermolecular interaction with the backbone carboxylate of Gt_α, i.e., that of F350. This is concurrent with the establishment of a salt bridge between E247(6.30) of rhodopsin and K345 of Gt_α (Fig. 4).

This interaction pattern is the most reliable one regardless of the side chain conformations of $Gt_{\alpha\beta}$, as well as of the length and side chain/main chain conformations of Gt_γ. It is worth noting that wild type Gt_α and the $Gt_\alpha/Gi_{\alpha 1}$ chimera produced identical best complexes, consistent with their similar functional behavior [85].

Structural complementarity, reliability, and consistency with in vitro evidences all converged in the same rhodopsin-Gt complex, showing that the functionally important R135(3.50) of the E/DRY motif is almost accessible to the C-terminus of Gt_α already in the dark state. Collectively, and consistent with results from a number of in vitro experiments [78–82], the results of our computational experiments suggest that MII formation follows the pre-coupling between dark rhodopsin and heterotrimeric transducin [65].

Another noteworthy result is that the most reliable complex between monomeric rhodopsin and Gt is found also when dimeric or tetrameric rhodopsin is used as a target (D. Dell'Orco et al., manuscript in preparation). This suggests that the receptor monomer holds the structural determinants for G protein activation, consistent with the results of in vitro experiments [86].

Activation of rhodopsin and of Gt may be concurrent processes, consisting of conformational changes in a supramolecular complex formed prior to the light-induced activation of the photoreceptor. In this respect, the rhodopsin-Gt interaction model obtained from our experiments may be considered as the

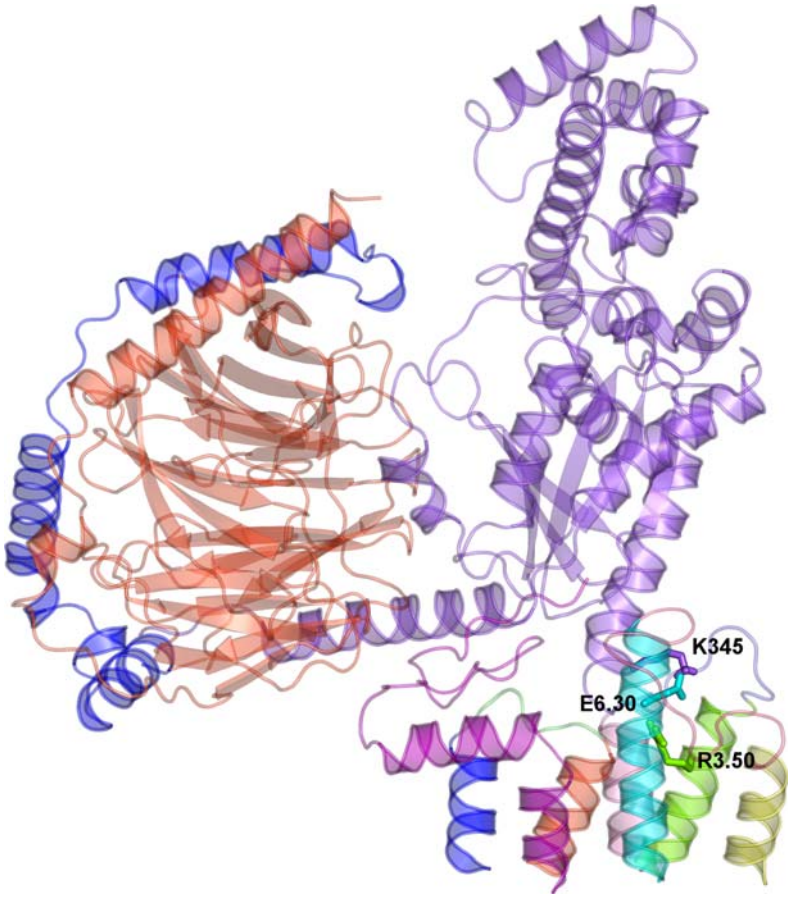

Fig. 4 View of one of the selected complexes between heterotrimeric Gt and dark rhodopsin, seen in a direction parallel to the putative membrane surface. The $Gt_{\alpha\beta\gamma}$ subunits are colored in violet, orange, and blue, respectively. As for rhodopsin, only the cytosolic half is shown. The helices and the cytosolic loops of the photoreceptor display different colors: H1–H7 are, respectively, colored in blue, orange, green, pink, yellow, cyan, and magenta. H8 and the C-tail are colored in magenta as well. The first, second and third intracellular loops are colored in lime, slate, and salmon, respectively. Sticks represent the side chains of R135(3.50) and E247(6.30), from rhodopsin, and of K345, from Gt_α. Drawings were done by means of the software PYMOL 0.97 (http://pymol.sourceforge.net/)

starting point for computational investigations of such processes.

We are currently exploring the receptor-G protein pre-coupling hypothesis and the putative receptor-G protein interface in a number of GPCRs including LHR, thyroid stimulating hormone (TSH) receptor, δ-opioid receptor and thromboxane A2 receptor. Preliminary results concerning wild type and CAM forms of LHR suggest that the most reliable solutions share the docking of the C-term of the α-subunit in between H3 and H6 of the receptor (K. Angelova et al., manuscript in preparation). In the D564(6.30)G CAM, the increase in solvent exposure of the E/DRY arginine results in a direct interaction between the highly conserved cationic amino acid and the C-term of Gs_{α}. A novel concept that is arising from these preliminary results is that constitutively active LHR mutants show improved complementarity for Gs compared to the wild type (K. Angelova et al., manuscript in preparation).

Conclusions and perspectives

The entirety of our computational studies have been devoted to inferring the structural features shared in common by active and non-active receptor states induced either by ligand or by mutation. When possible, molecular descriptors were defined and used for in silico screening of novel receptor ligands or novel receptor mutants.

The extensive computational and in vitro experiments on substantially different GPCRs, such as the α_{1b}-AR, LHR, and OTR, allowed us to infer hypotheses on the requirements for a GPCR site to be susceptible to activating mutations, highlighting commonalties and differences among the distinct mutation sites. One inference from computations was that, despite the topological and physico-chemical differences between them, the activating mutation sites are structurally connected with peculiar portions of the cytosolic domains, including the E/DRY motif. In fact, activating mutations tend to weaken the ground state interactions of R143(3.50) and increase the solvent accessibility of selected amino acids at the cytosolic extensions of H3 and H6. This structural effect is suggested to be mediated by highly conserved polar amino acids in the 7-helix bundle. Very recent docking simulations between wild type and CAM forms of the LHR and heterotrimeric Gs provided new insights into the features of mutation-induced active forms, i.e., receptor states characterized by better complementarity for the G protein compared to the non-active ones.

Similarly to the active states induced by mutation, the final target of the structural modifications induced by activating ligands is the interface between H3 and H6 holding the arginine of the E/DRY motif. Whether the main role of the E/DRY arginine is to maintain the inactive state of the receptor or to recognize the G protein is not clearly understood and may depend on the receptor system (critically analyzed in refs. [87, 88]) For some GPCRs, like the α_{1b}-AR [39], OTR [53], and the novel receptor ORF74-EHV2 [89], in which the ad hoc engineered or spontaneous absence of the E/DRY arginine is associated with constitutive activity that is abolished in the presence of the DR pair, the main role of the conserved arginine may be to maintain the inactive state of the receptor and drive receptor isomerization into different functional states (reviewed also in ref. [88]).

For the ligands that dock into the 7-helix bundle, the information transfer from the ligand binding site to the cytosolic interface between H3 and H6 is triggered by a few critical intermolecular interactions and appears to be mediated by a cluster of aromatic amino acids in H6 that undergo a conformational change associated with a reduction in the bend at P6.50. The results of our studies suggest that the role of GPCR ligands cannot be limited to a selection of pre-existing receptor conformations. They should rather dictate novel conformational states unlikely to be explored by the empty wild-type receptor.

Interestingly, even if either activating mutations or activating ligands induce the weakening of the R3.50-E6.30 salt bridge, no dramatic detachment between the cytosolic ends of these two helices was ever shown by the active-state structures [22–24, 29, 48, 52], inconsistent with inferences from biophysical experiments on rhodopsin activation [90]. The high-resolution structure of activated rhodopsin is needed to validate or dispel the low-resolution information from biophysical experiments.

The convergence of the results of computational experiments conducted under different conditions (i.e., restrained and unrestrained MD, in vacuo or using implicit water/membrane models) and on different receptor systems provides strength to the inferences from the study, which relies on an extensive comparative analysis aimed at inferring similarity/differences within the same approximations. One of the main inferences is that a GPCR exists in different active and inactive states that, however, share a few key structural features, which presumably determine the macroscopic functional receptor state.

An important aspect of our approach is that, as soon as novel high-resolution information or new

computational tools and algorithms become available, we critically revise the computational setup in order to improve the reliability of the computational models. In this respect, we are evaluating the effectiveness of a number of implicit membrane models [91–93].

We are also exploring the role of the internal water molecules into the structural features of the inactive an active receptor states. This is expected to provide insight into the role of polar conserved amino acids that, in the latest released structure of rhodopsin, are involved in a water-mediated H-bonding network [94].

The challenge of future computational modeling approaches is to provide a stochastic description of the GPCR systems and to predict, at the atomic level, the mechanisms by which structural information is transferred from the extracellular to the intracellular site of the same receptor molecule (i.e., intramolecular communication), within a molecular network of receptors, or within a multi-component signaling unit (i.e., intermolecular communication). This would require an extensive integration between different molecular simulation methods and a careful consideration of the approximations.

Acknowledgments This study was supported by a Telethon-Italy grant n. TCP00068 and NIH grant DK033973 (To FF).

References

1. Bockaert J, Pin JP (1999) Embo J 18:1723
2. Gether U (2000) Endocr Rev 21:90
3. Lefkowitz RJ (2000) Nat Cell Biol 2:E133
4. Pierce KL, Premont RT, Lefkowitz RJ (2002) Nat Rev Mol Cell Biol 3:639
5. Kristiansen K (2004) Pharmacol Ther 103:21
6. Bouvier M (2001) Nat Rev Neurosci 2:274
7. Milligan G (2001) J Cell Sci 114:1265
8. Rios CD, Jordan BA, Gomes I, Devi LA (2001) Pharmacol Ther 92:71
9. George SR, O'Dowd BF, Lee SP (2002) Nat Rev Drug Discov 1:808
10. Agnati LF, Ferre S, Lluis C, Franco R, Fuxe K (2003) Pharmacol Rev 55:509
11. Franco R, Canals M, Marcellino D, Ferre S, Agnati L, Mallol J, Casado V, Ciruela F, Fuxe K, Lluis C, Canela EI (2003) Trends Biochem Sci 28:238
12. Kroeger KM, Pfleger KD, Eidne KA (2003) Front Neuroendocrinol 24:254
13. Terrillon S, Bouvier M (2004) EMBO Rep 5:30
14. Park PS, Filipek S, Wells JW, Palczewski K (2004) Biochemistry 43:15643
15. Maggio R, Novi F, Scarselli M, Corsini GU (2005) Febs J 272:2939
16. Bulenger S, Marullo S, Bouvier M (2005) Trends Pharmacol Sci 26:131
17. Brady AE, Limbird LE (2002) Cell Signal 14:297
18. Freire E (2000) Proc Natl Acad Sci USA 97:11680
19. Onaran HO, Scheer A, Cotecchia S, Costa T (2000) In: Kenakin T, Angus J (eds) Handbook of experimental pharmacology. Springer, Heidelberg, pp 217–280
20. Kenakin T (2002) Nat Rev Drug Discov 1:103
21. Palczewski K, Kumasaka T, Hori T, Behnke CA, Motoshima H, Fox BA, Le Trong I, Teller DC, Okada T, Stenkamp RE, Yamamoto M, Miyano M (2000) Science 289:739
22. Fanelli F, De Benedetti PG (2005) Chem Rev 105:3297
23. Greasley PJ, Fanelli F, Rossier O, Abuin L, Cotecchia S (2002) Mol Pharmacol 61:1025
24. Greasley PJ, Fanelli F, Scheer A, Abuin L, Nenniger-Tosato M, DeBenedetti PG, Cotecchia S (2001) J Biol Chem 276:46485
25. Shinozaki H, Fanelli F, Liu X, Jaquette J, Nakamura K, Segaloff DL (2001) Mol Endocrinol 15:972
26. Fanelli F, Themmen AP, Puett D (2001) IUBMB Life 51:149
27. Fanelli F, Puett D (2002) Endocrine 18:285
28. Angelova K, Fanelli F, Puett D (2002) J Biol Chem 277:32202
29. Fanelli F, Verhoef-Post M, Timmerman M, Zeilemaker A, Martens JW. Themmen AP (2004) Mol Endocrinol 18:1499
30. Zhang M, Mizrachi D, Fanelli F, Segaloff DL (2005) J Biol Chem 280:26169
31. Favre N, Fanelli F, Missotten M, Nichols A, Wilson J, Di Tiani M, Rommel C, Scheer A (2005) Biochemistry 44:9990
32. Ascoli M, Fanelli F, Segaloff DL (2002) Endocr Rev 23:141
33. Fanelli F (2000) J Mol Biol 296:1333
34. Fanelli F, Menziani C, Scheer A, Cotecchia S, De Benedetti PG (1999) Proteins 37:145
35. Fanelli F, Menziani MC, Scheer A, Cotecchia S, De Benedetti P (1999) Int J Quantum Chem 73:71
36. Scheer A, Fanelli F, Costa T, De Benedetti PG, Cotecchia S (1997) Proc Natl Acad Sci USA 94:808
37. Scheer A, Fanelli F, Costa T, De Benedetti PG, Cotecchia S (1996) Embo J 15:3566
38. Fanelli F, Menziani MC, Scheer A, Cotecchia S, De Benedetti PG (1998) Methods 14:302
39. Scheer A, Costa T, Fanelli F, De Benedetti PG, Mhaouty-Kodja S, Abuin L, Nenniger-Tosato M, Cotecchia S (2000) Mol Pharmacol 57:219
40. Ballesteros JA, Weinstein H (1995) Methods Neurosci 25:366
41. Kjelsberg MA, Cotecchia S, Ostrowski J, Caron MG, Lefkowitz RJ (1992) J Biol Chem 267:1430
42. Fanelli F, Menziani MC, De Benedetti PG (1995) Bioorg Med Chem 3:1465
43. Fanelli F, Menziani MC, De Benedetti PG (1995) Protein Eng 8:557
44. Okada T, Ernst OP, Palczewski K, Hofmann KP (2001) Trends Biochem Sci 26:318
45. Ballesteros JA, Jensen AD, Liapakis G, Rasmussen SG, Shi L, Gether U, Javitch JA (2001) J Biol Chem 276:29171
46. Visiers I, Ebersole B, Dracheva S, Ballesteros J, Sealfon SC, Weinstein H (2002) Int J Quantum Chem 88:65
47. Shapiro DA, Kristiansen K, Weiner DM, Kroeze WK, Roth BL (2002) J Biol Chem 277:11441
48. Seeber M, De Benedetti PG, Fanelli F (2003) J Chem Inf Comput Sci 43:1520
49. Vassart G, Pardo L, Costagliola S (2004) Trends Biochem Sci 29:119
50. Mirzadegan T, Benko G, Filipek S, Palczewski K (2003) Biochemistry 42:2759
51. Huang P, Li J, Chen C, Visiers I, Weinstein H, Liu-Chen LY (2001) Biochemistry 40:13501
52. Vitale RM, Pedone C, De Benedetti PG Fanelli F (2004) Proteins 56:430

53. Fanelli F, Barbier P, Zanchetta D, De Benedetti PG, Chini B (1999) Mol Pharmacol 56:214
54. Lin SW, Sakmar TP (1996) Biochemistry 35:11149
55. Shi L, Liapakis G, Xu R, Guarnieri F, Ballesteros JA, Javitch JA (2002) J Biol Chem 277:40989
56. Singh R, Hurst DP, Barnett-Norris J, Lynch DL, Reggio PH, Guarnieri F (2002) J Pept Res 60:357
57. Gouldson PR, Kidley NJ, Bywater RP, Psaroudakis G, Brooks HD, Diaz C, Shire D, Reynolds CA (2004) Proteins 56:67
58. Sansom MS, Weinstein H (2000) Trends Pharmacol Sci 21:445
59. Fritze O, Filipek S, Kuksa V, Palczewski K, Hofmann KP, Ernst OP (2003) Proc Natl Acad Sci USA 100:2290
60. Onaran HO, Costa T (1997) Ann NY Acad Sci 812:98
61. Canals M, Marcellino D, Fanelli F, Ciruela F, De Benedetti P, Goldberg SR, Neve K, Fuxe K, Agnati LF, Woods AS, Ferre S, Lluis C, Bouvier M Franco R (2003) J Biol Chem 278:46741
62. Casciari D, Seeber M, Fanelli F (2006) BMC Bioinformatics 7:340
63. Fanelli F (2006) Molecular and Cellular Endocrinology, accepted for publication
64. Dell'Orco D, Seeber M, De Benedetti P, Fanelli F (2005) J Chem Inf Mod 45:1429
65. Fanelli F, Dell'Orco D (2005) Biochemistry 44:14695
66. Fanelli F, Ferrari S (2006) J Struct Biol 153:278
67. Dean MK, Higgs C, Smith RE, Bywater RP, Snell CR, Scott PD, Upton GJ, Howe TJ, Reynolds CA (2001) J Med Chem 44:4595
68. del Sol Mesa A, Pazos F, Valencia A (2003) J Mol Biol 326:1289
69. Filizola M, Weinstein H (2005) Febs J 272:2926
70. Nemoto W, Toh H (2005) Proteins 58:644
71. Soyer OS, Dimmic MW, Neubig RR, Goldstein RA (2003) Biochemistry 42:14522
72. Thummer RP, Campbell MP, Dean MK, Frusher MJ, Scott PD, Reynolds CA (2005) J Mol Neurosci 26:113
73. Chen R, Weng Z (2003) Proteins 51:397
74. Liang Y, Fotiadis D, Filipek S, Saperstein DA, Palczewski K, Engel A (2003) J Biol Chem 278:21655
75. Ciruela F, Burgueno J, Casado V, Canals M, Marcellino D, Goldberg SR, Bader M, Fuxe K, Agnati LF, Lluis C, Franco R, Ferre S, Woods AS (2004) Anal Chem 76:5354
76. Canals M, Burgueno J, Marcellino D, Cabello N, Canela EI, Mallol J, Agnati L, Ferre S, Bouvier M, Fuxe K, Ciruela F, Lluis C, Franco R (2004) J Neurochem 88:726
77. Guo W, Filizola M, Weinstein H, Javitch JA (2005) Proc Natl Acad Sci USA 102:17495
78. Hamm HE, Deretic D, Hofmann KP, Schleicher A, Kohl B (1987) J Biol Chem 262:10831
79. Alves ID, Salgado GF, Salamon Z, Brown MF, Tollin G, Hruby VJ (2005) Biophys J 88:198
80. Fahmy K, Sakmar TP, Siebert F (2000) Biochemistry 39:10607
81. Salamon Z, Wang Y, Soulages JL, Brown MF, Tollin G (1996) Biophys J 71:283
82. Wang X, Kim SH, Ablonczy Z, Crouch RK, Knapp DR (2004) Biochemistry 43:11153
83. Okada T, Sugihara M, Bondar AN, Elstner M, Entel P, Buss V (2004) J Mol Biol 342:571
84. Chen R, Li L, Weng Z (2003) Proteins 52:80
85. Lambright DG, Sondek J, Bohm J, Skiba NP, Hamm HE, Sigler PB (1996) Nature 379:311
86. Chabre M, le Maire M (2005) Biochemistry 44:9395
87. Capra V, Veltri A, Foglia C, Crimaldi L, Habib A, Parenti M, Rovati GE (2004) Mol Pharmacol 66:880
88. Flanagan CA (2005) Mol Pharmacol 68:1
89. Rosenkilde MM, Kledal TN, Schwartz TW (2005) Mol Pharmacol 68:11
90. Farrens DL, Altenbach C, Yang K, Hubbell WL, Khorana HG (1996) Science 274:768
91. Im W, Feig M, Brooks CL III (2003) Biophys J 85:2900
92. Lazaridis T (2003) Proteins 52:176
93. Spassov VZ, Yan L, Szalma S (2002) J Phys Chem B 106:8726
94. Okada T (2004) Biochem Soc Trans 32:738